

Fabrication and characterization of amorphous lithium electrolyte thin films and rechargeable thin-film batteries

J. B. Bates, N. J. Dudney, G. R. Gruzalski, R. A. Zuhr, A. Choudhury and C. F. Luck

Oak Ridge National Laboratory, Oak Ridge, TN 37830 (USA)

J. D. Robertson

Department of Chemistry, University of Kentucky, Lexington, KY 40506 (USA)

Abstract

Amorphous oxide and oxynitride lithium electrolyte thin films were synthesized by r.f. magnetron sputtering of lithium silicates and lithium phosphates in Ar, Ar+O₂, Ar+N₂, or N₂. The composition, structure, and electrical properties of the films were characterized using ion and electron beam, X-ray, optical, photoelectron, and a.c. impedance techniques. For the lithium phosphosilicate films, lithium ion conductivities as high as 1.4×10^{-6} S/cm at 25 °C were observed, but none of these films selected for extended testing were stable in contact with lithium. On the other hand, a new thin-film lithium phosphorus oxynitride electrolyte, synthesized by sputtering Li₃PO₄ in pure N₂, was found to have a conductivity of 2×10^{-6} S/cm at 25 °C and excellent long-term stability in contact with lithium. Thin-film cells consisting of a 1 μm thick amorphous V₂O₅ cathode, a 1 μm thick oxynitride electrolyte film, and a 5 μm thick lithium anode were cycled between 3.7 and 1.5 V using discharge rates of up to 100 μA/cm² and charge rates of up to 20 μA/cm². The open-circuit voltage of 3.6 to 3.7 V of fully-charged cells remained virtually unchanged after months of storage.

Introduction

Research of the deposition and characterization of amorphous lithium electrolyte and vanadium oxide thin films was undertaken with the goal of developing a thin-film rechargeable Li battery. Most of this effort has been focused on finding an inorganic electrolyte that is stable in thin-film Li cells.

The electrolyte for a thin-film rechargeable Li battery should ideally have a high Li ion conductivity and a negligible electronic conductivity, but it must also be stable in contact with Li at cell potentials of several V. While many inorganic and polymeric electrolytes have satisfactory electrical properties, their degradation in contact with Li precludes their application in a Li cell. Because of the intrinsic stress that may be present in the electrolyte film and because it is deposited over the cathode and portions of the current collectors, resulting in steps with high-stress regions, the electrolyte must be resistant to cracking and to decohesion from the cathode and substrate. Films deposited by sputtering or evaporation of inorganic compounds onto substrates held at ambient temperatures are usually amorphous. This is advantageous because for many Li compounds, the Li ion conductivity of the amorphous phase is

orders of magnitude higher than that of the crystalline phase. In thin-film form, the conductance of the amorphous film is often adequate for use as an electrolyte. Thus there is a wide choice of materials available for possible application in thin-film cells. Recent studies of a newly-discovered electrolyte, lithium phosphorus oxynitride, and rechargeable thin-film cells using this electrolyte with vanadium oxide cathodes and Li anodes are discussed in this paper.

Experimental procedures

Amorphous oxide and oxynitride films about $1\ \mu\text{m}$ thick were deposited by single- and dual-source r.f. magnetron sputtering of Li_3PO_4 , Li_4SiO_4 , Li_3PO_4 - Li_4SiO_4 mixtures, Li_2O , and SiO_2 in Ar, Ar + O_2 , Ar + N_2 , or pure N_2 . Details of the deposition process and target preparation are described elsewhere [1-4]. For each film grown, a portion of the film was deposited over several types of substrates, e.g., sapphire, graphite, alumina, and glass, as required for the various characterization experiments.

The compositions of the films were determined using a variety of ion beam, electron beam, and spectroscopic techniques to obtain accurate analyses. For the phosphosilicate and oxynitride films, the Li:P and/or Li:Si ratios were obtained from proton-induced gamma-ray emission (PIGE) analysis [5] and atomic-emission spectrometry, and the relative P and Si contents were determined from Rutherford backscattering spectrometry (RBS) and X-ray microanalysis (EDX) [2]. In addition, for the lithium phosphorus oxynitride (Lipon) films, nuclear resonance ion backscattering and X-ray photoelectron (XPS) and Auger electron spectroscopies were used to determine the N content. Ionic conductivities of the films were obtained from a.c. impedance measurements on symmetric Au/electrolyte/Au sandwich structures fabricated on alumina substrates. The measurements were made at frequencies from 0.1 Hz to 10 MHz and at temperatures from 25 to 120 °C [6].

Vanadium oxide films were deposited by d.c. magnetron sputtering of V in 20 mTorr of 14% O_2 in Ar at flow rates of 10 and 20 cm^3/s . The structure of the films was investigated using grazing angle X-ray diffraction, Raman scattering acquired with a microprobe and the 514.5 nm line of an argon laser, and scanning electron microscopy (SEM). The amorphous films were yellow on transparent substrates, whereas the crystalline films with the fibrous microstructure described below were red.

Lithium cells were fabricated on glass substrates that had been prepared by depositing $0.5\ \mu\text{m}$ thick V films near the center and edge of the substrate to serve as current collectors. A $1\ \text{cm}^2$ film of vanadium oxide about $1\ \mu\text{m}$ thick was deposited onto the larger of the current collectors, and the cathode film was then covered by a $2\ \text{cm}^2 \times 1\ \mu\text{m}$ thick electrolyte film. Lastly, a $1\ \text{cm}^2 \times 3$ - $5\ \mu\text{m}$ thick Li film, with a narrow strip extending to the V current collector, was deposited over the electrolyte by thermal evaporation of Li. Schematic diagrams of the cell in cross section and in plan view are shown Fig. 1. Thin-film Li cells also were fabricated using the Lipon electrolyte and cathodes of TiS_2 prepared at Eveready Battery Co., [7] and Li_xCoO_2 prepared at Tufts University [8]. Using Keithley 617 electrometers operated under computer control, the cells were cycled at constant current between preset voltage limits and held at these limits at the end of each charge or discharge cycle until the current dropped below a preset value, usually less than 10% of the charge or discharge current. Impedance measurements (0.01 Hz to 10 MHz) were made on several of the Li- V_2O_5 cells at intermediate stages of the charge/discharge cycle between 3.7 and 1.5 V and on the Li- TiS_2 and Li- Li_xCoO_2 cells at high and low charge states.

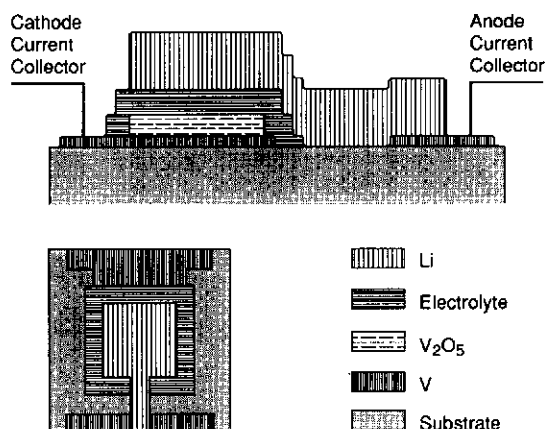


Fig. 1. Schematic drawings of the thin-film battery in cross-section and plan view. The cathode and electrolyte films are about $1 \mu\text{m}$ thick, and the lithium anode film is about $5 \mu\text{m}$ thick.

TABLE 1

Comparison of the compositions, conductivities, and activation energies of amorphous lithium phosphate, phosphosilicate, and phosphorous oxynitride electrolyte films

Target	Process gas	Film composition	$\sigma \times 10^8$, at 25°C (S/cm)	E_a^* (eV)
Li_3PO_4	40% O_2 in Ar	$\text{Li}_{2.7}\text{PO}_{3.9}$	7	0.68
$\text{Li}_3\text{PO}_4 + \text{Li}_4\text{SiO}_4$	40% O_2 in Ar	$\text{Li}_{3.6}(\text{Si}_{0.19}\text{P}_{0.82})\text{O}_{4.2}$	20	0.57
Li_3PO_4	N_2	$\text{Li}_{3.1}\text{PO}_{3.8}\text{N}_{0.16}$	200	0.57
Li_3PO_4	N_2	$\text{Li}_{3.3}\text{PO}_{3.8}\text{N}_{0.22}$	240	0.56
Li_3PO_4	N_2	$\text{Li}_{2.9}\text{PO}_{3.3}\text{N}_{0.46}$	330	0.54

*Determined from a least squares fit of $\sigma T = \sigma_0 \exp(-E_a/kT)$ to conductivity data.

Results and discussion

The conductivities, σ , at 25°C and activation energies, E_a , for several compositions are given in Table 1. The activation energies were determined from least squares fitting of the Arrhenius equation, $\sigma T = \sigma_0 \exp(-E_a/kT)$, to the conductivities measured at different temperatures. The lithium phosphosilicate listed had the highest conductivity of the films in the $\text{Li}_2\text{O}:\text{SiO}_2:\text{P}_2\text{O}_5$ system. However, conductivities higher than 2×10^{-6} S/cm at 25°C were observed in the films deposited by sputtering Li_3PO_4 in pure N_2 . This is more than 30 times greater than the conductivity of the films deposited by sputtering Li_3PO_4 in 40% O_2 in Ar.

The cause of this increase in σ is not fully understood, but it is believed to be due to an increase in Li ion mobility brought about by a change in the structure of the electrolyte. The N 1s photoelectron spectrum obtained from an oxynitride film is shown in Fig. 2. The asymmetric peak near 397.5 eV was resolved into two peaks at

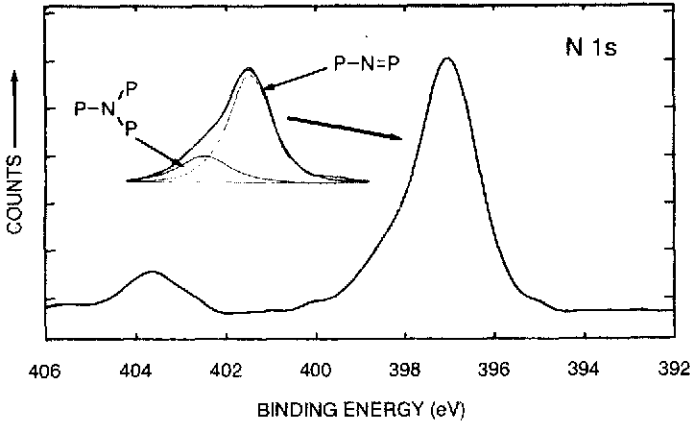


Fig. 2. X-ray photoelectron spectrum in the region of the N 1s peaks in $\text{Li}_{2.9}\text{PO}_{3.3}\text{N}_{0.46}$.

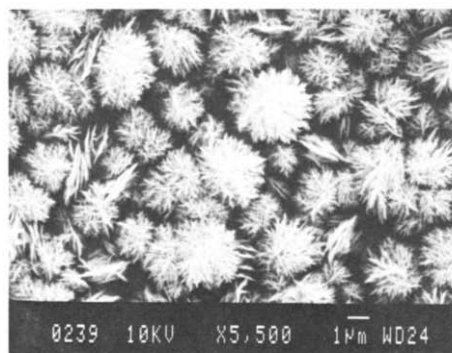
397.4 and 398.9 eV (inset in Fig. 2). These are close to similarly resolved features at 397.8 and 399.3 eV assigned to N bound as P-N=P and as $\text{P-N}\begin{smallmatrix} \text{P} \\ \text{P} \end{smallmatrix}$, respectively, from XPS measurements on nitrated bulk sodium metaphosphate glasses [9]. The weaker photoelectron peak near 404 eV (Fig. 2) is possibly due to N bound in O-N=O groups [10]. The formation of the cross-linked $\text{P-N}\begin{smallmatrix} \text{P} \\ \text{P} \end{smallmatrix}$ structure might be responsible for the increase in the mobility of the Li^+ ions. Large conductivity increases were also observed when Si was incorporated into $\text{Li}_2\text{O-P}_2\text{O}_5$ films resulting in cross-linked structures by the formation of $-\text{Si-O-P}-$ bonds. Based on the relative intensities of the resolved N 1s components at 397.4 and 398.9 eV (Fig. 2), about 20% of the N in the films is bound as $\text{P-N}\begin{smallmatrix} \text{P} \\ \text{P} \end{smallmatrix}$, and so about 30% of the P atoms in the film are bound in these cross-linked structures. A comparison of the oxynitrides in Table 1 suggests that films with more N have higher conductivities; however, the uncertainty in the N analysis is not known at this time. It is interesting to note that although the films are deposited by sputtering Li_3PO_4 in pure N_2 , none of them contain more than about 6 at.% N.

The incorporation of N into the electrolyte thin films not only increased their conductivity but, more importantly, improved their electrochemical stability. Prior to our synthesis of the LiPON, $\text{Li-V}_2\text{O}_5$ cells fabricated with several of the most conductive of the $\text{Li}_2\text{O-SiO}_2\text{-P}_2\text{O}_5$ electrolytes were not stable. Cells fabricated with the oxynitride electrolyte, however, appear to be stable indefinitely, exhibiting only a small voltage loss which is assumed to be due to the electronic conductivity of the electrolyte (estimated at $\sim 10^{13} \Omega \text{ cm}$). At present, the lifetime of the cells is limited by a gradual degradation of the Li anode from exposure to residual N_2 in our glove box. One of the Li/LiPON/TiS_2 cells, which has an open-circuit voltage of about 2.5 V at full charge, has undergone over 4000 charge/discharge cycles since fabrication in July, 1991 [7]. Two recently-fabricated $\text{Li/LiPON/Li}_x\text{CoO}_2$ cells exhibited open-circuit voltages of 4.4

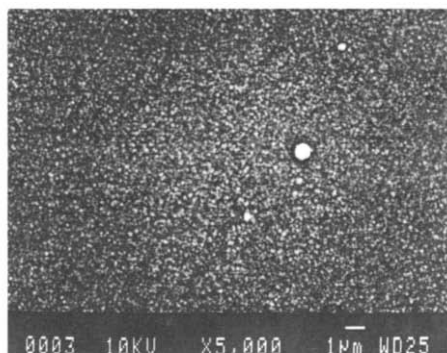
and 4.2 V, respectively. As of this writing, the 4.2 V cell has undergone 15 cycles between 3 and 4.8 V at charge and discharge current densities of 3 and 10 $\mu\text{A}/\text{cm}^2$, respectively. Because of the high resistance of the cathodes in these cells, the current densities for charge and discharge were reduced to 0.05 and 0.1 $\mu\text{A}/\text{cm}^2$, respectively, for cycling of the 4.4 V cell. The results with the TiS_2 and Li_xCoO_2 cells clearly demonstrate the long-term stability of the lithium phosphorus electrolyte in contact with Li and the electrochemical stability of Lipon at high cell potentials.

Thin films of V_2O_5 have been deposited by evaporation of V_2O_5 [11], r.f. and d.c. reactive sputtering of V [12, 13], and r.f. sputtering of V_2O_5 [14]. Films deposited by reactive sputtering of V in $\text{Ar} + \text{O}_2$ onto ambient temperature or cooled substrates were amorphous and had a yellow color whenever the concentration of O_2 in the process gas exceeded about 8 to 10% [12, 13]. On the other hand, the films deposited by sputtering V_2O_5 in Ar and $\text{Ar} + \text{O}_2$ were partly crystalline and had variable colors from orange to black [14]. The microstructure of these amorphous and crystalline films were not described in any of these earlier papers.

We have found that vanadium oxide films deposited by d.c. magnetron sputtering of 1 inch V targets in 20 mTorr of 14% O_2 in Ar at a total flow rate of about 10 cm^3/s are characterized by a high density of micron-sized fibrous clusters as shown in the SEM micrograph in Fig. 3(a). These films were identified as crystalline V_2O_5 by grazing angle X-ray diffraction and Raman scattering measurements [1]. When the flow rate was increased to about 20 cm^3/s and when the V target was relatively new, the films were smooth on a submicron scale as shown in Fig. 3(b), and no diffraction peaks were observed in grazing angle X-ray measurements suggesting that the films were amorphous. Auger measurements on these films yield a composition that is within a few percent of V_2O_5 , and Raman spectra of these films were also consistent with an amorphous V_2O_5 structure [15]. As the V target aged by extended sputtering, the microstructure of the films deposited with the higher flow rate gradually evolved to that of the films deposited at the lower flow rate. With continued use of the same target, the density of the fibrous clusters gradually increased as illustrated by the micrographs in Fig. 4. This change in the microstructure of the films was marked by a decrease in target voltage (at constant power) and a decrease in the deposition rate



(a)



(b)

Fig. 3. Micrographs of V_2O_5 films: (a) film deposited at a flow rate of 10 sccm, and (b) film deposited at a flow rate of 20 sccm using a fresh V target.

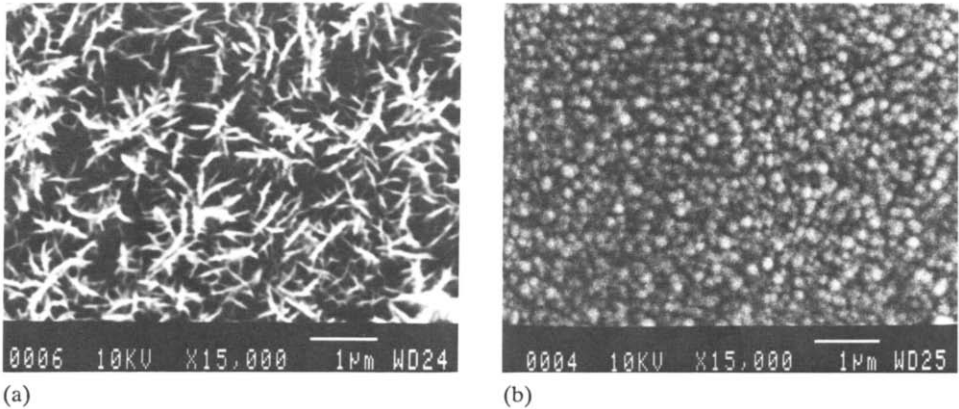


Fig. 4. Micrographs of V_2O_5 films: (a) aged V target, and (b) new V target.

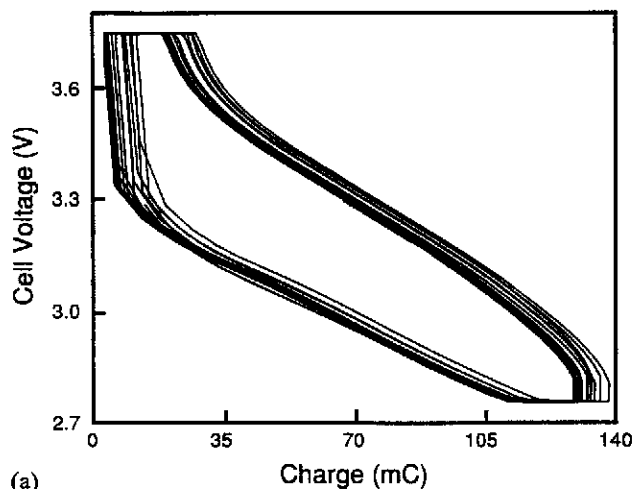
by nearly 50%. To regain the smooth amorphous form, a fresh V target (or target face) was required.

Cells fabricated with the crystalline or amorphous V_2O_5 cathodes had open-circuit voltages of 3.7 to 3.8 V. However, the rates of discharge and charge that the cells with the crystalline cathodes (Fig. 3(a)) could sustain without excessive polarization were significantly lower than the cells with amorphous cathodes, less than $10 \mu A/cm^2$ on the initial discharge and less than $1 \mu A/cm^2$ on the subsequent charge. This is believed to be due to poor transport across the electrolyte-cathode interface and through the fibrous structure. Micrographs of the interface show that the electrolyte does not conformally coat the rough microstructure of the crystalline cathodes [1]. Rather it covers just to top portion of the fibrous clusters, resulting in a relatively small contact area.

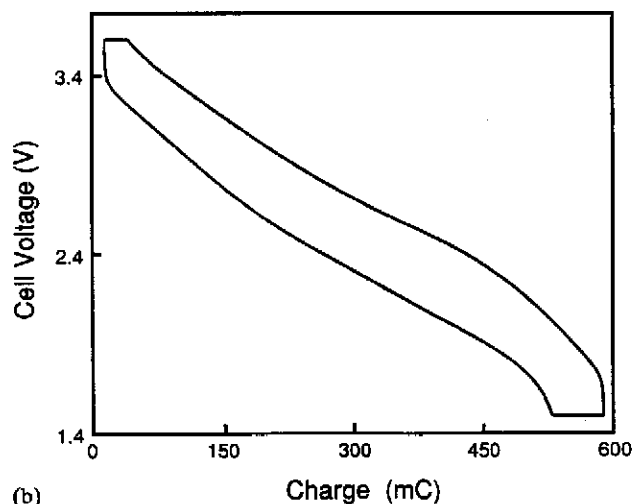
Cells fabricated with the smooth amorphous cathodes, on the other hand, were discharged at rates of up to $100 \mu A/cm^2$. Examples of charge/discharge curves for a cell cycled between 3.75 and 2.75 V and a cell cycled between 3.6 and 1.5 V are shown in Fig. 5. The abrupt drop in cell voltage from about 3.7 to about 3.4 V is due to an internal resistance of approximately $20 k\Omega$. Impedance measurements at different cell voltages suggest that this resistance is due to the cathode. In one set of measurements, as a cell was discharged, the internal resistance decreased from $< 10^5 \Omega$ at an open-circuit voltage of 3.7 V to about 2700Ω at an open-circuit voltage of 1.7 V. With continued discharge, the cell resistance increased again.

For a cathode about $1 \mu m$ thick, the cell capacity is approximately $120 mC/cm^2$ for discharge from 3.7 to 2.8 V and about $470 mC/cm^2$ for discharge from 3.6 to 1.5 V. The latter corresponds to a cathode composition of $Li_{2.5}V_2O_5$. Based on the masses of the cathode, electrolyte, and anode films, the specific energy and energy density are about $300 W h/kg$ and $360 W h/l$, respectively. If the thickness of the anode is reduced from ten times overcapacity to three times overcapacity, these values increase to about $400 W h/kg$ and $570 W h/l$, respectively.

There are a potentially many applications for a rechargeable thin-film battery as a backup or main power supply for microelectronic devices. Applications of the cells



(a)



(b)

Fig. 5. Discharge/charge curves for two Li/Lipon/ V_2O_5 cells: (a) cycles 17–23 between 3.75 and 2.75 V at discharge and charge current densities of $20 \mu A/cm^2$ and $5 \mu A/cm^2$, respectively, and (b) cycle 8 between 3.6 and 1.5 V at discharge and charge current densities of $15 \mu A/cm^2$ and $5 \mu A/cm^2$, respectively.

described above await the development of a technique to protect the Li anode from corrosion on exposure to air.

Acknowledgement

Research sponsored by the Division of Materials Sciences, US Department of Energy, under contract DE-AC05-84OR21400 with Martin Marietta Energy Systems, Inc.

References

- 1 J. B. Bates, N. J. Dudney, C. F. Luck and L. Klatt, *Ceram. Trans.*, 11 (1990) 35.
- 2 J. B. Bates, N. J. Dudney, B. C. Sales, J. D. Robertson, R. A. Zuhr, G. R. Gruzalski and C. F. Luck, *Proc. Material Research Society Symp.*, 1991, PV-2, p. 569.
- 3 N. J. Dudney, J. B. Bates, A. L. Wachs, J. D. Robertson and C. F. Luck, *Proc. Material Research Society Symp.*, 1991, PV-2, p. 579.
- 4 N. J. Dudney, J. B. Bates, R. A. Zuhr, C. F. Luck and J. D. Robertson, *Solid State Ionics*, 53-56 (1992) 655.
- 5 J. D. Robertson, J. B. Bates, N. J. Dudney and R. A. Zuhr, *Nucl. Instrum. Methods*, B56/57 (1991) 722.
- 6 J. B. Bates, N. J. Dudney, G. R. Gruzalski, R. A. Zuhr, A. Choudhury, C. F. Luck and J. D. Robertson, *Solid State Ionics*, 53-56 (1992) 647.
- 7 S. D. Jones, personal communication.
- 8 R. A. Goldner, personal communication.
- 9 R. Marchand, D. Agliz, L. Boukbir and A. Quemerais, *J. Non-Cryst. Solids*, 103 (1988) 35.
- 10 C. D. Wagner, W. M. Riggs, L. E. Davis and J. F. Moulder, in G. E. Muilenberg (ed.), *Handbook of X-ray Photoelectron Spectroscopy*, Perkin-Elmer Corporation, Eden Prairie, MN, 1979, p. 40.
- 11 R. J. Colton, A. M. Guzman and J. W. Rabalais, *J. Appl. Phys.*, 49 (1978) 409.
- 12 S. D. Hanson and C. R. Aita, *J. Vac. Sci. Technol. A*, 3 (1985) 660.
- 13 D. Wruck, S. Ramamurthi and M. Rubin, *Thin Solid Films*, 182 (1989) 79.
- 14 K. West, F. W. Poulsen, B. Zachau-Christiansen and S. V. Skarrup, *Solid State Ionics*, in press.
- 15 C. Sanchez, J. Livage and G. Lucazeau, *J. Raman Spectrosc.*, 12 (1982) 68.